Network EM Algorithm for Gaussian Mixture Model in Decentralized Federated Learning

Shuyuan Wu¹, Bin Du², Xuetong Li*³, and Hansheng Wang³

¹School of Statistics and Management, Shanghai University of Finance and
Economics, Shanghai, China; ²School of Statistics, Beijing Normal University,
Beijing, China; ³Guanghua School of Management, Peking University, Beijing, China

Abstract

We systematically study various network Expectation-Maximization (EM) algorithms for the Gaussian mixture model within the framework of decentralized federated learning. Our theoretical investigation reveals that directly extending the classical decentralized supervised learning method to the EM algorithm (Dempster et al., 1977) exhibits poor estimation accuracy with heterogeneous data across clients and struggles to converge numerically when Gaussian components are poorly-separated. To address these issues, we propose two novel solutions. First, to handle heterogeneous data, we introduce a momentum network EM (MNEM) algorithm, which uses a momentum parameter to combine information from both the current and historical estimators. Second, to tackle the challenge of poorly-separated Gaussian components, we develop a semi-supervised MNEM (semi-MNEM) algorithm, which leverages partially labeled data. Rigorous theoretical analysis demonstrates that MNEM can achieve statistical efficiency comparable to that of the whole sample estimator when the mixture components satisfy certain separation conditions, even in heterogeneous scenarios. Moreover, the semi-MNEM estimator enhances the convergence speed of the MNEM algorithm, effectively addressing the numerical convergence challenges in poorly-separated scenarios. Extensive simulation and real data analyses are conducted to justify our theoretical findings.

KEYWORDS: Decentralized Federated Learning; Distributed Computing; Semi-supervised Learning; Expectation-Maximization Algorithm; Gaussian Mixture Model.

^{*}Xuetong Li (2001110929@stu.pku.edu.cn) is the corresponding author.

1. INTRODUCTION

Massive data is commonly encountered in modern statistical analysis (Jordan et al., 2019; Hector and Song, 2021; Zhu et al., 2021; Fan et al., 2023). To analyze such data, appropriate computation systems and supporting algorithms are critically important. In this regard, federated learning (McMahan et al., 2017), a novel paradigm that trains a global model using data distributed across a large number of low-end devices (or clients) for collective learning, has gained increasing popularity. This approach not only utilizes the entire dataset on all these devices simultaneously for collective learning, but also leverages their distributed computational power. The primary challenge lies in learning the global model in ways that are both statistically efficient and privacy-preserving (Konečný et al., 2016).

To address this challenge, researchers have developed various federated learning algorithms (McMahan et al., 2017; Sattler et al., 2019; Li et al., 2019a; Liu et al., 2020; Marfoq et al., 2021; Fang and Ye, 2022; Tian et al., 2023). Classical federated learning algorithms are centralized algorithms. They assume the presence of a central computer connected to every client and train the global model iteratively. In each iteration, each client uses its local data to update the local estimator, based on some initial estimator provided by the central computer. The updated local estimators are then collected and aggregated by the central computer. Next, the resulting aggregated estimators are broadcast back to each local client to serve as the initial estimators for the next round of local updates. Under certain regularity conditions, each client's estimator gradually stabilizes and converges (Li et al., 2020; Chen et al., 2022). Moreover, since the client transmits parameter estimators rather than raw data during the update process, concerns over privacy disclosures are significantly mitigated.

Despite their usefulness, centralized federated learning algorithms are criticized for

several reasons. First, they have a high bandwidth requirement: the central machine must communicate with a large number of clients (Li et al., 2021). Second, centralized systems are vulnerable: if the central computer stops operating, then the entire system shuts down (Liu et al., 2022). Lastly, centralized systems are sub-optimal for privacy protection: once the central computer is attacked, the attacker can communicate with all clients (Bellet et al., 2018). To address these limitations, researchers have proposed decentralized federated learning (DFL), which operates without central computers (Blot et al., 2016; Yuan et al., 2016; Stich, 2018; Li et al., 2019a; Liu et al., 2020; Li et al., 2020; Tang et al., 2024). Specifically, the training of DFL is distributed among multiple clients in a communication-based network, where each client functions as a node and the connections between clients are treated as directed edges. During each training iteration, each client collects and aggregates the estimators from their one-hop neighbors (i.e., directly followed neighbors) in the network. Subsequently, local updates are conducted based on the resulting aggregated estimator.

Most existing DFL works focus on solving supervised learning problems using gradient-based algorithms (such as stochastic gradient descent). They demonstrated that, under certain conditions, the resulting estimator can be as statistically efficient as the whole sample estimator, i.e., the estimator obtained by aggregating all data on a single machine (Shi et al., 2015); see also Gabrielli et al. (2023) for a comprehensive review. While these analyses are useful, they are constrained by a common requirement – namely the need for precisely observed class labels. However, meeting this requirement is not always feasible. For example, in machine learning tasks such as image classification, while a large number of images can be easily obtained using digital cameras, labeling these images is time-consuming and labor-intensive, requiring significant human effort. For instance, automated pulmonary nodule diagnosis requires a vast collection of CT images annotated with nodule positions for training (Zhou et al., 2023).

This requires hiring multiple experienced radiologists who must expend considerable effort to manually create these annotations across different hospitals or institutions. Thus, it becomes crucial to study unsupervised and semi-supervised learning with large volumes of unlabeled data under the DFL framework.

In this paper, we develop novel DFL algorithms designed for fitting the Gaussian mixture model (GMM, McLachlan and Basford, 1988). Due to its clear definition and wide applicability (Gu, 2008; Reynolds et al., 2009; Boldea and Magnus, 2009; Yang et al., 2012; Heinrich and Kahn, 2018; McLachlan et al., 2019; Zhang and Chen, 2022), we believe GMM serves as an appropriate starting point for exploring unsupervised and semi-supervised learning problems within DFL.

Our contribution lies in developing various DFL-type expectation maximization (EM) algorithms and analyzing their statistical properties. Specifically:

- We first analyze a naïve network EM (NNEM) algorithm that directly applies the supervised DFL algorithm to the EM for fitting GMMs. Our theoretical analysis reveals that (i) When data is heterogeneous, the resulting estimator is significantly biased. (ii) When the Gaussian components are poorly-separated, this algorithm struggles to converge numerically. To address these limitations, we propose two alternative DFL-type EM algorithms, elaborated in the next two bullet points.
- To handle heterogeneous data, we propose a momentum network expectation maximization (MNEM) algorithm, which combines information from both current and historical estimators. We theoretically prove that the MNEM algorithm can attain the oracle property, i.e., achieving the same asymptotic efficiency as the whole sample estimator, provided the momentum parameter is sufficiently small and the Gaussian components satisfy certain separation conditions.
- To handle poorly-seperated Gaussian components, we propose a semi-supervised

MNEM (semi-MNEM) algorithm using partially labeled data. We theoretically demonstrate that the semi-MNEM converges faster than MNEM and achieves the oracle property even when the Gaussian components are poorly-separated.

The rest of the paper is organized as follows. Section 2 introduces the GMM model, presents the NNEM algorithm and discusses its limitations. Section 3 introduces the proposed MNEM and semi-MNEM algorithms for fitting unsupervised and semi-supervised settings, respectively, along with their theoretical properties. Section 4 presents simulation experiments and a real data example. Finally, Section 5 concludes the paper with a brief discussion. All technical details are given in the Appendix.

2. MODEL SETUP

This paper studies GMM under the DFL framework across a variety of scenarios, where the setting can be either fully unsupervised or semi-supervised, and the data generating process can be either homogeneous or heterogeneous. This section is structured as follows. Section 2.1 introduces the GMM model under the two different settings. Section 2.2 introduces the two data generating processes, presents the NNEM algorithm, and demonstrates its limitation with heterogeneous data. Finally, Section 2.3 connects the degrees of separation of the Gaussian components with the convergence of EM algorithm and illustrates NNEM's failure with poorly-separated Gaussian components.

2.1. Two Settings for GMMs and the EM algorithm

The GMM model can be described using two random variables: (i) A categorical variable $Y \in \{1, \dots, K\}$ that specifies the label of the Gaussian component, with $\mathbb{P}(Y = k) = \alpha_k$ representing the mixing probability for the kth component such that $\sum_{k=1}^{K} \alpha_k = k$

1; (ii) A p-dimensional vector X whose conditional distribution given Y = k is Gaussian. We denote the mean and covariance matrix of this Gaussian distribution by $\mu_k \in \mathbb{R}^p$ and $\Sigma_k \in \mathbb{R}^{p \times p}$, respectively. The model parameter can be summarized into a vector $\theta_0 \in \mathbb{R}^q$ with $q = K(p^2 + 3p + 2)/2$, which consists of the collection of α_k , μ_k and vech (Σ_k) for k ranging from 1 to K. Here, vech $(A) = (A_{ij} : 1 \le i \le j \le p) \in \mathbb{R}^{p(p+1)/2}$ for any symmetric square matrix $A \in \mathbb{R}^{p \times p}$.

We consider two settings in this paper. In the fully unsupervised learning setting, the label Y is unknown, and the observed data consists of X_1, \dots, X_N that follow the aforementioned model, where N denotes the sample size. The negative log-likelihood function for the parameter is given by

$$\mathcal{L}(\theta) = -\frac{1}{N} \sum_{i=1}^{N} \log f(X_i | \theta) = -\frac{1}{N} \sum_{i=1}^{N} \log \left\{ \sum_{k=1}^{K} \alpha_k \phi_{\mu_k, \Sigma_k} (X_i) \right\}, \tag{2.1}$$

where $\phi_{\mu,\Sigma}$ denotes the Gaussian density function with mean vector μ and covariance matrix Σ . Accordingly, a maximum likelihood estimator (MLE) can be defined as $\widehat{\theta} = \operatorname{argmin} \mathcal{L}(\theta)$. Unfortunately, this estimator is not well defined without further constraint. This is mainly because the objective function $\mathcal{L}(\theta)$ is unbounded for $\theta \in \mathbb{R}^q$; see for example Boldea and Magnus (2009) and Zhang and Chen (2022) for some discussion. To fix the problem, one typical strategy is to work on a constrained parameter space Θ , which is locally around the true parameter θ_0 . We therefore redefine $\widehat{\theta} = (\widehat{\alpha}_k, (\widehat{\mu}_k)^{\mathsf{T}}, \operatorname{vech}^{\mathsf{T}}(\widehat{\Sigma}_k); k = 1, \dots, K)^{\mathsf{T}} = \operatorname{argmin}_{\theta \in \Theta} \mathcal{L}(\theta)$ for some sufficiently small but fixed local compact region with the true parameter. Classic literature suggests that $\widehat{\theta}$ should be strongly consistent and asymptotically efficient of θ_0 (Kiefer, 1978; Hathaway, 1985).

In the semi-supervised learning setting, we assume the existence of a subset of subjects $S^* \subseteq S = \{1, 2, \dots, N\}$ where both the feature X_i and the label Y_i are observed.

For instance, labels may be provided by the domain experts. This leads to the following negative log-likelihood function:

$$\mathcal{L}_{\text{semi}}(\theta) = -\frac{1}{N} \sum_{i \notin \mathcal{S}^*} \log f(X_i | \theta) - \frac{1}{N} \sum_{i \in \mathcal{S}^*} \sum_{k=1}^K \mathbb{I}(Y_i = k) \Big\{ \log \phi_{\mu_k, \Sigma_k}(X_i) + \log \alpha_k \Big\},$$

where $\mathbb{I}(\cdot)$ denotes the indicator function. The corresponding MLE can be computed by $\widehat{\theta}_{\text{semi}} = \operatorname{argmax}_{\theta \in \Theta} \mathcal{L}_{\text{semi}}(\theta)$.

To compute $\widehat{\theta}$ and $\widehat{\theta}_{\text{semi}}$ for GMM, a standard EM algorithm can be employed (Dempster et al., 1977; Xu, 1993; Cozman et al., 2003). The EM algorithm operates by iteratively alternating between estimating the latent variables and updating the parameter estimates, thereby gradually improving the likelihood function. The numerical convergence of EM for GMM has been extensively studied in the literature. Its local convergence can be guaranteed under certain conditions (Wu, 1983). Additionally, compared to classic gradient descent methods, the EM algorithm typically converges faster. Sometimes, a superlinear convergence rate can be achieved when the different Gaussian components are well-separated (Xu and Jordan, 1996; Ma et al., 2000).

2.2. Two Data Generating Processes and the NNEM Algorithm

In the DFL framework, data is distributed across different clients subject to privacy constraints, making it impractical to directly apply the EM algorithm. Therefore, we explore how to develop DFL-type EM algorithms in this paper. To this end, we first introduce two data generation processes in DFL:

1. Homogeneous process: Data is independently and identically distributed across different clients. In this scenario, local estimators across different clients converge to the same population limit, enabling the final estimator to achieve desirable statistical properties. This scenario has been extensively explored in the divide and

conquer literature (see e.g., Zhang et al., 2013; Chen and Xie, 2014; Shi et al., 2018a; Volgushev et al., 2019).

2. Heterogeneous process: Data is independently distributed across clients, but follow different distributions. In this scenario, due to the data heterogeneity, the local estimator on each client is biased. Such bias poses significant challenges in achieving accurate and reliable estimations (Shi et al., 2015; Yuan et al., 2016; Wu et al., 2023).

In this paper, we primarily focus on the second scenario, since it is commonly encountered in real-world applications (Shi et al., 2018b; Li et al., 2019a, 2020; Kairouz et al., 2021; Han et al., 2021; Xiang et al., 2024).

Next, we propose a naïve extension of the EM algorithm to the DFL setting and discuss its limitation in handling heterogeneous data. Assume the whole dataset is distributed among a total of M clients. We collect the indices of the sample allocated to the mth client by $\mathcal{S}_m \subset \mathcal{S}$. Consequently, we have $\mathcal{S} = \bigcup_{m=1}^M \mathcal{S}_m$ and $\mathcal{S}_{m_1} \cap \mathcal{S}_{m_2} = \emptyset$ for any $m_1 \neq m_2$. These clients are connected by a communication network $A = (a_{m_1 m_2}) \in \mathbb{R}^{M \times M}$, where $a_{m_1 m_2} = 1$ if client m_1 can receive information from m_2 , and $a_{m_1 m_2} = 0$ otherwise. By normalizing A, we obtain the weighting matrix $W = (w_{m_1 m_2}) \in \mathbb{R}^{M \times M}$ with $w_{m_1 m_2} = a_{m_1 m_2} / \sum_{m_2} a_{m_1 m_2}$. For simplicity, we assume $|\mathcal{S}_m| = n$ for every $1 \leq m \leq M$ so that the data is evenly distributed among all clients.

To minimize $\mathcal{L}(\theta)$ in a decentralized setting, we can adapt classical decentralized gradient descent methods (Colin et al., 2016; Yuan et al., 2016; Lian et al., 2017) to the EM algorithm. This yields the Naïve Network Expectation Maximization (NNEM) algorithm, summarized in Algorithm 1. The key idea of the NNEM algorithm is for each client to update its local parameter estimator based on estimators collected from its neighbors, along with its own local data. Specifically, during each iteration, each client first aggregates all estimators from its one-hop neighbors through a simple

Algorithm 1: Naïve Network Expectation Maximization Algorithm[†]

Input: Initial estimators $\widehat{\theta}^{(0,m)} = (\widehat{\alpha}_k^{(0,m)}, (\widehat{\mu}_k^{(0,m)})^{\mathsf{T}}, \text{vech}^{\mathsf{T}}(\widehat{\Sigma}_k^{(0,m)}); k = 1, \dots, K)^{\mathsf{T}}$ on the mth client, weighting matrix W, maximum iterations T;

Output: $\widehat{\theta}^{(T,m)}$ on the mth client;

while $\underline{t < T}$ do

for $\underline{m = 1, 2, \dots, M}$ (distributedly) do

for $\underline{k = 1, 2, \dots, K}$ do

Compute the neighborhood-averaged estimator $\widehat{\alpha}_k^{(t,m)} = \sum_{q=1}^M w_{mq} \widehat{\alpha}_k^{(t,q)}; \widetilde{\mu}_k^{(t,m)} = \sum_{q=1}^M w_{mq} \widehat{\mu}_k^{(t,q)};$ $\widehat{\Sigma}_k^{(t,m)} = \sum_{q=1}^M w_{mq} \widehat{\Sigma}_k^{(t,q)};$ $\widehat{\Sigma}_k^{(t,m)} = \sum_{q=1}^M w_{mq} \widehat{\Sigma}_k^{(t,q)};$ (2.2)

Update the local parameter estimator $\widehat{\alpha}_{k}^{(t+1,m)} = \sum_{i \in \mathcal{S}_{m}} \widetilde{\pi}_{ik}^{(t,m)} / n; \widehat{\mu}_{k}^{(t+1,m)} = n^{-1} \sum_{i \in \mathcal{S}_{m}} \widetilde{\pi}_{ik}^{(t,m)} X_{i} / \widehat{\alpha}_{k}^{(t+1,m)};$

$$\widehat{\Sigma}_k^{(t+1,m)} = n^{-1} \sum_{i \in \mathcal{S}_m} \widetilde{\pi}_{ik}^{(t,m)} \Big(X_i - \widetilde{\mu}_k^{(t,m)} \Big) \Big(X_i - \widetilde{\mu}_k^{(t,m)} \Big)^{\mathsf{T}} / \widehat{\alpha}_k^{(t+1,m)};$$

(2.3)

Here
$$\widetilde{\pi}_{ik}^{(t,m)} = f^{-1} \Big(X_i | \widetilde{\theta}_k^{(t,m)} \Big) \widetilde{\alpha}_k^{(t,m)} \phi_{\widetilde{\mu}_k^{(t,m)}, \widetilde{\Sigma}_k^{(t,m)}} (X_i).$$

t = t + 1;

average. Next, this neighborhood-averaged estimator is updated using the local data via an E-step and an M-step.

The NNEM method is easy to describe and implement. It can also be proven that NNEM achieves consistent estimation under stringent conditions, requiring homogeneous data distribution and well-separated Gaussian components. This interesting finding can be explained theoretically. The relevant theory is to be provided in Section 2.4. Nevertheless, the following analysis suggests that the NNEM estimator might be largely biased with highly heterogeneous data. To illustrate this idea, consider the following toy example.

[†]We remove all the "nnem" subscripts for ease of notation.

A Toy Example: Consider a simple univariate GMM with only two components and two clients. In other words, we assume that $X_i \in \mathbb{R}$, K = 2, and M = 2. We further assume known variances $\Sigma_1 = \Sigma_2 = 1$, equal mixing probabilities $\alpha_1 = \alpha_2 = 0.5$, and remarkably different means $\mu_1 = -\mu_2 = 1$. Next, consider an extremely heterogeneous data distribution with all positive data allocated to the first client and the remaining non-positive data assigned to the second client. According to Equations (2.2) and (2.3), it follows that $\widehat{\mu}_k^{(t,1)} > 0$ and $\widehat{\mu}_k^{(t,2)} \le 0$ for every $1 \le k \le 2$ and $1 \le t \le T$, since $\widehat{\pi}_{ik}^{(t,m)} \ge 0$ for any k, m, t. Therefore, the first client's estimator for $\mu_2 = -1$ is given by $\widehat{\mu}_2^{(t,1)} > 0$, which is seriously biased. Similarly, the second client's estimator for $\mu_1 = 1$ is given by $\widehat{\mu}_1^{(t,2)} \le 0$, demonstrating large bias as well.

2.3. Degree of Separation and Numerical Convergence in NNEM

As discussed in Section 2.2, data heterogeneity poses a critical challenge for the NNEM. In this section, we detail the second challenge for the NNEM, brought by poorly-separated Gaussian components. To begin with, we define a metric $\tau_k = \mathbb{E}\{\pi_k(1-\pi_k)\}$ with $\pi_k = f^{-1}(x|\theta_0)\alpha_k\phi_{\mu_k,\Sigma_k}(x)$. Intuitively, a small τ_k value suggests that samples belonging to the kth component can be easily distinguished from those of other components based on π_{ik} s. Conversely, a large τ_k value indicates that the kth component is difficult to separate from other components by X_i s. Consequently, this τ_k metric characterizes the degree of separation of the kth Gaussian component. We find that the degree of separation plays a crucial role in the numerical convergence of the classical EM algorithm for solving GMMs. Specifically, if different Gaussian components are difficult to distinguish from each other, the algorithm might fail to converge (Regev and Vijayaraghavan, 2017; Kwon and Caramanis, 2020).

To detail the impact of separability on the classical EM algorithm's convergence properties, we introduce some notations. Define $\widehat{\theta}^{(t)} \in \mathbb{R}^q$ as the EM estimator for θ_0

derived in the tth iteration. We represent the updating formula for the EM algorithm by $\widehat{\theta}^{(t+1)} = F(\widehat{\theta}^{(t)})$ with the detailed definition of F given in Appendix. Notably, $\widehat{\theta}$ is a stable solution of the EM algorithm and a fixed point of the mapping F, satisfying $\widehat{\theta} = F(\widehat{\theta})$. Additionally, $\widehat{\theta}$ is consistent, leading to $\widehat{\theta} \approx \theta_0$. This allows us to apply Taylor's expansion to obtain the following asymptotic approximation,

$$\widehat{\theta}^{(t+1)} - \widehat{\theta} = F(\widehat{\theta}^{(t)}) - F(\widehat{\theta}) \approx \dot{F}(\theta_0) (\widehat{\theta}^{(t)} - \widehat{\theta}), \tag{2.4}$$

where $\dot{F}(\theta_0)$ represents the first-order derivative of $F(\cdot)$ with respect to θ_0 . We refer to $\dot{F}(\theta_0)$ as a contraction operator. By equation (2.4), $\dot{F}(\theta_0)$ is crucial for the numerical convergence of the EM algorithm. Define $\rho(A)$ as the spectral radius of any matrix A. The following theorem demonstrates the relationship between this contraction operator and the degree of separation.

Theorem 1. Assume that X_1, \ldots, X_N are identically and independently generated from a GMM model (2.1) with parameter θ_0 . Then we have: (i) $||\dot{F}(\theta_0)|| \leq C_0 \max_k \sqrt{\tau_k}$ with probability at least $1 - O(N^{-\alpha})$ for any $\alpha \geq 1$ and some positive constant C_0 ; and (ii) $\rho(\dot{F}(\theta_0)) \rightarrow_p 1$ as $\tau_k \rightarrow \alpha_k (1 - \alpha_k)$ for every $1 \leq k \leq K$.

According to Theorem 1, we find that the numerical convergence of the algorithm is significantly affected by the degree of separation of Gaussian components through the τ_k -metric. In general, better separation leads to a smaller $\|\dot{F}(\theta_0)\|$, which in turn results in faster convergence. Conversely, a relatively larger τ_k , indicating poorly-separated Gaussian components, makes convergence more difficult. Consider an extreme situation with $\mu_k = \mu$ and $\Sigma_k = \Sigma$ for some $\mu \in \mathbb{R}^p$ and $\Sigma \in \mathbb{R}^{p \times p}$, and every $1 \le k \le K$. In this case, the mixture components are perfectly overlapped. Therefore, $\pi_{ik} = P(Y_i = k|X_i) = P(Y_i = k) = \alpha_k$. If this happens, we find that $\rho\{\dot{F}(\theta_0)\} = 1$. This suggests that the algorithm fails to converge. Notice that the above analysis specifically applies to the

classical EM algorithm. However, it is reasonable to expect that with poorly-separated Gaussian components, NNEM, which adapts classical EM to the DFL setting, also struggles to achieve convergence.

2.4. NNEM in the Most Ideal Situation

In the previous analysis, we demonstrated that the NNEM estimator may struggle in both heterogeneous and poorly-separated cases. However, it remains unclear what would happen in the most ideal scenario. This ideal scenario refers to a situation with sufficiently small τ_k and homogeneous mixture components. To address this theoretical gap, we develop this subsection. To this end, define $\widehat{\theta}_{nnem}^{(t,m)}$ as the NNEM estimator obtained on the m-th client in the t-th stage. The updating formula of the NNEM algorithm can then be simplified to $\widehat{\theta}_{nnem}^{(t+1,m)} = F_{(m)}(\widetilde{\theta}_{nnem}^{(t,m)})$, where $\widetilde{\theta}_{nnem}^{(t,m)} = \sum_{q=1}^{M} w_{mq} \widehat{\theta}_{nnem}^{(t,q)}$ and $F_{(m)}(\cdot)$ is a mapping function defined as follows:

$$F_{(m)\Sigma_k}(\theta) = \left(\sum_{i \in \mathcal{S}_m} \pi_{ik}\right)^{-1} \sum_{i \in \mathcal{S}_m} \pi_{ik} \operatorname{vech}\left\{ (X_i - \mu_k)(X_i - \mu_k)^{\top} \right\} \in \mathbb{R}^{(p+1)p/2},$$

$$F_{(m)\mu_k}(\theta) = \left(\sum_{i \in \mathcal{S}_m} \pi_{ik}\right)^{-1} \sum_{i \in \mathcal{S}_m} \pi_{ik} X_i \in \mathbb{R}^p,$$

$$F_{(m)\alpha_k}(\theta) = n^{-1} \sum_{i \in \mathcal{S}_m} \pi_{ik} \in \mathbb{R}.$$

In the homogeneous case, we should be able to derive a locally consistent estimator on each client. Specifically, we should expect that the loss function $\mathcal{L}_{(m)}(\theta)$ has a unique local minimum $\widehat{\theta}_{\text{loc}}^{(m)}$ that serves as a consistent and asymptotically efficient estimator of θ_0 . Then, by setting $\widehat{\theta}_{\text{nnem}}^{*(t)} = \{(\widehat{\theta}_{\text{nnem}}^{(t,1)})^{\mathsf{T}}, \dots, (\widehat{\theta}_{\text{nnem}}^{(t,M)})^{\mathsf{T}}\}^{\mathsf{T}} \in \mathbb{R}^{Mq}$, the NNEM algorithm can be rewritten as

$$\widehat{\theta}_{\text{nnem}}^{*(t+1)} - \widehat{\theta}_{\text{loc}}^{*} = \dot{F}^{*(t)} \left\{ (W \otimes I_q) \widehat{\theta}_{\text{nnem}}^{*(t)} - \widehat{\theta}_{\text{loc}}^{*} \right\}.$$
 (2.5)

Here $\dot{F}^{*(t)} = \operatorname{diag}\{\dot{F}_{(1)}(\widetilde{\xi}_{nnem}^{(t,1)}), \ldots, \dot{F}_{(M)}(\widetilde{\xi}_{nnem}^{(t,M)})\} \in \mathbb{R}^{Mq \times Mq}$ represents the contraction operator, where $\dot{F}_{(m)}(\widetilde{\xi}_{nnem}^{(t,m)}) = \{\dot{F}_{(m),1}^{\top}(\widetilde{\xi}_{nnem,1}^{(t,m)}); \ldots; \dot{F}_{(m),q}^{\top}(\widetilde{\xi}_{nnem,q}^{(t,m)})\} \in \mathbb{R}^{q \times q}, \ \dot{F}_{(m),j}(\cdot) \text{ is the } j\text{-th row of } \dot{F}_{(m)}(\cdot), \text{ and } \widetilde{\xi}_{nnem,j}^{(t,m)} \in \mathbb{R}^q \text{ lies on the line joining } \widetilde{\theta}_{nnem}^{(t,m)} \text{ and } \widehat{\theta}_{loc}^{(m)}.$ Equation (2.5) holds because $\widehat{\theta}_{loc}^{(m)} = F_{(m)}(\widehat{\theta}_{loc}^{(m)})$. Based on (2.5), we can rigorously describe the discrepancy between the NNEM estimator and the local optimal estimator.

Subsequently, let $B(\theta_0, \delta) = \{\theta' \in \mathbb{R}^q | \|\theta' - \psi_0\| \le \delta\}$ be a sphere with a center θ_0 and a radius $\delta > 0$. Before presenting the formal results of the theorem, we should consider the following regularity conditions.

- (C1) (PARAMETER SPACE) Assume the parameter space Θ is a compact and convex subset of \mathbb{R}^q . $\theta_0 \in \operatorname{int}(\Theta)$ and $\delta = \sup_{\theta' \in \Theta} \|\theta' \theta_0\|$ is some sufficiently small but fixed constant.
- (C2) (SMOOTHNESS) Define $B(\theta_0, \delta) = \{\theta' \in \mathbb{R}^p | \|\theta' \theta_0\| \le \delta\} \subset \Theta$ to be a sphere with a center θ_0 and a radius $\delta > 0$. For any $1 \le m \le M$, there exists some positive constant L_{\max} such that $\|\mathbb{E}\{\dot{F}_{(m)}(\theta')\}\| \le L_{\max}$ for any $\theta' \in B(\theta_0, \delta)$.

Conditions (C1) and (C2) are classical regularity conditions in convex optimization; see for example Zhang et al. (2013), Jordan et al. (2019) for more details. Let $\widehat{\delta}_{\max}^0 = \max_{m} \|\widehat{\theta}_{\text{nnem}}^{(0,m)} - \widehat{\theta}_{\text{loc}}^{(m)}\|$ be the initial distance. Define $\theta_0^* = I_M^* \theta_0$ as the stacked true estimator, where $I^* = \mathbf{1}_M \otimes I_q \in \mathbb{R}^{M \times q}$, and $\mathbf{1}_M = (1, \dots, 1)^{\mathsf{T}} \in \mathbb{R}^M$. We then have the following Theorem.

Theorem 2. Assume conditions (C1) and (C2) hold, further assume that: (i) the local data $\{X_i\}_{i\in\mathcal{S}_m}$ are independently and identically distributed across different clients, and (ii) there exists a sufficiently small but fixed positive constant ϵ , such that $\max_k \tau_k \leq \epsilon$, and the initial value $\widehat{\theta}_{\text{nnem}}^{*(0)}$ is sufficiently close to θ_0^* in the sense $\|\widehat{\theta}_{\text{nnem}}^{(0,m)} - \theta_0\| \leq \epsilon$ for

every $1 \le m \le M$. Then we have

$$\frac{\|\widehat{\theta}_{\text{nnem}}^{*(t)} - \widehat{\theta}_{\text{loc}}^{*}\|}{\sqrt{M}} \le \widehat{\delta}_{\text{max}}^{0} \rho_{\text{max}}^{t} + C_{1} \left\{ \max_{m} \|\widehat{\theta}_{\text{loc}}^{(m)} - \theta_{0}\| + \sqrt{\max_{k} \tau_{k}} \right\} \frac{\|\widehat{\theta}_{\text{loc}}^{*} - \theta_{0}^{*}\|}{\sqrt{M}}$$
(2.6)

holds with probability at least $1 - O(Mn^{-\alpha})$ for any $\alpha \ge 1$ and some constants $C_1 > 0$ and $0 < \rho_{\max} < 1$. Here C_1 is related to α but are independent of $(\max_k \tau_k, n, M)$. In particular, if $\max_k \tau_k \to 0$ as $n \to \infty$, we have $\lim_{t\to\infty} M^{-1/2} \|\widehat{\theta}_{nnem}^{*(t)} - \widehat{\theta}_{loc}^{*}\| = o_p(n^{-1/2})$.

By the theorem conclusion (2.6), we know that the discrepancy between $\widehat{\theta}_{\text{nnem}}^{*(t)}$ and $\widehat{\theta}_{\text{loc}}^{*}$ could be decomposed into two parts. The first part is the numerical error $\widehat{\delta}_{\text{max}}^{0} \rho_{\text{max}}^{t}$, which converges linearly to 0 as $t \to \infty$. The second part is the statistical error, which is of order $o_p(n^{-1/2})$ as $\max_k \tau_k \to 0$. As a result, the NNEM estimator is asymptotically equivalent to $\widehat{\theta}_{\text{loc}}^{*}$ in this special case. Note that $\widehat{\theta}_{\text{loc}}^{*}$ is a sub-optimal efficient estimator compared with the whole sample estimator $\widehat{\theta}$. This indicates that even for this most ideal case, the NNEM estimator cannot achieve optimal statistical efficiency.

3. METHODOLOGY

As discussed in Sections 2, extending the EM algorithm to the DFL setting faces two major challenges: data heterogeneity and poorly-separated Gaussian components. In this section, we propose two novel DFL algorithms to address these challenges. This section is structured as follows: Section 3.1 introduces the proposed MNEM algorithm to correct the bias caused by data heterogeneity. Section 3.2 presents the semi-MNEM algorithm that leverages partially labeled data to improve numerical convergence in the presence of poorly-separated Gaussian components. We further study the theoretical properties of the two proposed algorithms in Sections 3.3 and 3.4, respectively.

3.1. Momentum Network EM Algorithm

In most decentralized gradient descent algorithms, the bias introduced by heterogeneous local data can be effectively mitigated by adjusting the selecting a sufficiently small learning rate parameter (Shi et al., 2015; Yuan et al., 2016). However, in the NNEM Algorithm outlined in Algorithm 1, both the E-step and M-step calculations utilize closed-form expressions. Consequently, there are no tuning parameters, such as learning rates, involved to approximate these expressions. As a result, we lose the opportunity to regulate the adverse effects of data heterogeneity. As we have demonstrated in the toy example, the parameter updating direction (i.e., the locally computed gradients) is largely affected by local data and can be strongly biased in each computation iteration.

The above discussion motivates the proposed momentum network EM algorithm for bias reduction. Different from the NNEM algorithm, MNEM incorporates an additional momentum parameter to combine information from both the current step and historical estimators. By assigning a smaller weight to the current step estimator, MNEM effectively alleviates the bias caused by data heterogeneity inherent in the current step estimator.

We next detail the MNEM algorithm, summarized in Algorithm 2. Let $\widehat{\theta}_{\text{mnem}}^{(t,m)} = (\widehat{\alpha}_{\text{mnem},k}^{(t,m)}, (\widehat{\mu}_{\text{mnem},k}^{(t,m)})^{\mathsf{T}}, \text{vech}^{\mathsf{T}} (\widehat{\Sigma}_{\text{mnem},k}^{(t,m)}); k = 1, \ldots, K)^{\mathsf{T}}$ denote the MNEM estimator obtained after the tth iteration on the mth client. Parameter updates for $\widehat{\theta}_{\text{mnem}}^{(t,m)}$ consist of two steps, which we detail below. Since the update formula is similar across all components, we focus on the kth component $(\widehat{\alpha}_{\text{mnem},k}^{(t,m)}, \widehat{\mu}_{\text{mnem},k}^{(t,m)}, \widehat{\Sigma}_{\text{mnem},k}^{(t,m)})$ for illustration.

STEP 1. Similar to the NNEM algorithm, each client updates the estimators by utilizing information from its neighbors. Here, we slightly modify the first step of the NNEM algorithm following Gu (2008) and Safarinejadian et al. (2010), which helps reduce bias. Specifically, each client calculates $\widehat{\beta}_{\text{mnem},k}^{(t,m)} = \widehat{\mu}_{\text{mnem},k}^{(t,m)} \widehat{\alpha}_{\text{mnem},k}^{(t,m)}$ and $\widehat{\gamma}_{\text{mnem},k}^{(t,m)} = \widehat{\Sigma}_{\text{mnem},k}^{(t,m)} \widehat{\alpha}_{\text{mnem},k}^{(t,m)}$, and passes these estimators rather than $\widehat{\mu}_{\text{mnem},k}^{(t,m)}$ and $\widehat{\Sigma}_{\text{mnem},k}^{(t,m)}$

to their neighbors to produce the neighbourhood-averaged estimators.

STEP 2. Each client utilizes local data to update the neighborhood-averaged estimator by a momentum EM algorithm, resulting in a weighted average of the updated estimator (i.e., current step estimator) and the neighborhood-averaged estimator (i.e., past estimator):

$$\widehat{\alpha}_{\text{mnem},k}^{(t+1,m)} = \frac{\eta}{n} \sum_{i \in \mathcal{S}_m} \widetilde{\pi}_{ik}^{(t,m)} + (1-\eta) \widetilde{\alpha}_{\text{mnem},k}^{(t,m)},$$

$$\widehat{\beta}_{\text{mnem},k}^{(t+1,m)} = \frac{\eta}{n} \sum_{i \in \mathcal{S}_m} \widetilde{\pi}_{ik}^{(t,m)} X_i + (1-\eta) \widetilde{\beta}_{\text{mnem},k}^{(t,m)},$$

$$\widehat{\gamma}_{\text{mnem},k}^{(t+1,m)} = \frac{\eta}{n} \sum_{i \in \mathcal{S}_m} \widetilde{\pi}_{ik}^{(t,m)} \left(X_i - \widetilde{\mu}_{\text{mnem},k}^{(t,m)} \right) \left(X_i - \widetilde{\mu}_{\text{mnem},k}^{(t,m)} \right)^{\mathsf{T}} + (1-\eta) \widetilde{\gamma}_{\text{mnem},k}^{(t,m)}.$$
(3.1)

Here $\eta > 0$ is the momentum parameter. The incorporation of η in MNEM substantially enhances its estimation accuracy when compared against NNEM. To illustrate this improvement, we revisit the toy example. Assuming $\widehat{\theta}_{\text{mnem}}^{(t,m)} \approx \theta_0$, Equation (3.1) shows that when η is sufficiently small, the estimator at t + 1th iteration will remain close to the true parameter, effectively mitigating the bias induced by heterogeneous data. More rigorous justifications will be provided in Section 3.3.

3.2. Semi-supervised MNEM Algorithm

The MNEM method developed in the previous subsection can effectively handle heterogeneous data. However, according to our analysis in Section 2.3, MNEM may still struggle to converge numerically if the Gaussian components are poorly-separated. To address this limitation, we further develop a semi-supervised MNEM algorithm in this section by utilizing partially labeled data. We refer to this new approach as the semi-MNEM.

Semi-MNEM is very similar to MNEM; the only difference lies in the utilization of

[‡]We remove all the "mnem" subscripts for ease of notation.

Algorithm 2: Momentum Network Expectation Maximization Algorithm[‡]

Input: Initial estimators
$$\widehat{\theta}^{(0,m)}$$
; $(\widehat{\beta}_k^{(0,m)} = \widehat{\mu}_k^{(0,m)} \widehat{\alpha}_k^{(0,m)},$
 $\widehat{\gamma}_k^{(0,m)} = \widehat{\Sigma}_k^{(0,m)} \widehat{\alpha}_k^{(0,m)}; k = 1, \dots, K)$ on the m th client, weighting matrix W , momentum parameter η , maximum iterations T ;

Output: $\widehat{\theta}^{(T,m)}$ on the mth client;

while t < T do

for
$$m = 1, 2, ..., M$$
 (distributedly) do for $k = 1, 2, ..., K$ do

Compute the neighborhood-averaged estimator
$$\widetilde{\beta}_{k}^{(t,m)} = \sum_{q=1}^{M} w_{mq} \widehat{\beta}_{k}^{(t,q)}; \widetilde{\gamma}_{k}^{(t,m)} = \sum_{q=1}^{M} w_{mq} \widehat{\gamma}_{k}^{(t,q)};$$

$$\widetilde{\alpha}_{k}^{(t,m)} = \sum_{q=1}^{M} w_{mq} \widehat{\alpha}_{k}^{(t,q)};$$
Update the local parameter estimator
$$\widetilde{\mu}_{k}^{(t,m)} = \widetilde{\beta}_{k}^{(t,m)} / \widetilde{\alpha}_{k}^{(t,m)}; \widetilde{\Sigma}_{k}^{(t,m)} = \widetilde{\gamma}_{k}^{(t,m)} / \widetilde{\alpha}_{k}^{(t,m)}, \text{ and }$$

$$\widetilde{\pi}_{ik}^{(t,m)} = f^{-1}(X_{i}|\widetilde{\theta}^{(t,m)}) \widetilde{\alpha}_{k}^{(t,m)} \phi_{\widetilde{\mu}_{k}^{(t,m)}, \widetilde{\Sigma}_{k}^{(t,m)}}(X_{i});$$
Update $(\widehat{\alpha}_{k}^{(t+1,m)}, \widehat{\beta}_{k}^{(t+1,m)}, \widehat{\gamma}_{k}^{(t+1,m)})$ by equation (3.1);

$$\widetilde{\mu}_{k}^{(t,m)} = \widetilde{\beta}_{k}^{(t,m)} / \widetilde{\alpha}_{k}^{(t,m)}; \widetilde{\Sigma}_{k}^{(t,m)} = \widetilde{\gamma}_{k}^{(t,m)} / \widetilde{\alpha}_{k}^{(t,m)}, \text{ and}$$

$$\widetilde{\pi}_{ik}^{(t,m)} = f^{-1}(X_{i} | \widetilde{\theta}^{(t,m)}) \widetilde{\alpha}_{k}^{(t,m)} \phi_{\widetilde{\mu}_{k}^{(t,m)}, \widetilde{\Sigma}_{k}^{(t,m)}}(X_{i});$$
Update $(\widehat{\alpha}_{k}^{(t+1,m)}, \widehat{\beta}_{k}^{(t+1,m)}, \widehat{\gamma}_{k}^{(t+1,m)})$ by equation (3.1)

labels to update the neighborhood-averaged estimator. Specifically, let $\mathcal{S}_m^* \subset \mathcal{S}^*$ be the index set of all labeled observations on the mth client. For simplicity, we assume that $|\mathcal{S}_m^*| = n^*$ for every $1 \le m \le M$. Define $\widehat{\theta}_{\text{snem}}^{(t,m)} = (\widehat{\alpha}_{\text{snem},k}^{(t,m)}, (\widehat{\mu}_{\text{snem},k}^{(t,m)})^{\mathsf{T}}, \text{vech}^{\mathsf{T}}(\widehat{\Sigma}_{\text{snem},k}^{(t,m)}); k = 0$ $[1,\ldots,K]^{\mathsf{T}} \in \mathbb{R}^q$ as the semi-MNEM estimator on the mth client at the tth iteration. We update $\widehat{\theta}_{\text{snem}}^{(t+1,m)}$ as follows:

$$\widehat{\alpha}_{\text{snem},k}^{(t+1,m)} = \frac{\eta}{n} \left\{ \sum_{i \in \mathcal{S}_m \setminus \mathcal{S}_m^*} \widetilde{\pi}_{ik}^{(t,m)} + \sum_{i \in \mathcal{S}_m^*} a_{ik} \right\} + (1 - \eta) \widetilde{\alpha}_{\text{snem},k}^{(t,m)},
\widehat{\beta}_{\text{snem},k}^{(t+1,m)} = \frac{\eta}{n} \left\{ \sum_{i \in \mathcal{S}_m \setminus \mathcal{S}_m^*} \widetilde{\pi}_{ik}^{(t,m)} X_i + \sum_{i \in \mathcal{S}_m^*} a_{ik} X_i \right\} + (1 - \eta) \widetilde{\beta}_{\text{snem},k}^{(t,m)},
\widehat{\gamma}_{\text{snem},k}^{(t+1,m)} = (1 - \eta) \widetilde{\gamma}_{\text{snem},k}^{(t,m)} + \frac{\eta}{n} \left\{ \sum_{i \in \mathcal{S}_m \setminus \mathcal{S}_m^*} \widetilde{\pi}_{ik}^{(t,m)} \left(X_i - \widetilde{\mu}_{\text{snem},k}^{(t,m)} \right) \left(X_i - \widetilde{\mu}_{\text{snem},k}^{(t,m)} \right)^{\mathsf{T}} \right.
+ \sum_{i \in \mathcal{S}_m^*} a_{ik} \left(X_i - \widetilde{\mu}_{\text{snem},k}^{(t,m)} \right) \left(X_i - \widetilde{\mu}_{\text{snem},k}^{(t,m)} \right)^{\mathsf{T}} \right\},$$
(3.2)

where $a_{ik} = \mathbb{I}(Y_i = k)$, and $\widetilde{\beta}_{\text{snem},k}^{(t,m)}$, $\widetilde{\gamma}_{\text{snem},k}^{(t,m)}$, $\widetilde{\alpha}_{\text{snem},k}^{(t,m)}$ are the neighborhood-averaged estimators. Compared to the local updating formulas of MNEM described in (3.1), those of semi-MNEM in (3.2) integrate information from both the features X_i and a_{ik} , which contains the label information. This integration leads to a contraction operator with a smaller spectral radius (see Section 3.4 for details), which substantially improves semi-MNEM's numerical convergence over MNEM, particularly in cases where the Gaussian components are poorly-separated. Further details of semi-MNEM are relegated Appendix.

3.3. Theoretical Properties of the MNEM

This section presents the theoretical properties of the MNEM estimator. Define $\widehat{\psi}_{\mathrm{mnem}}^{(t,m)} = (\widehat{\alpha}_{\mathrm{mnem},k}^{(t,m)}, (\widehat{\beta}_{\mathrm{mnem},k}^{(t,m)})^{\mathsf{T}}, \mathrm{vech}^{\mathsf{T}}(\widehat{\gamma}_{\mathrm{mnem},k}^{(t,m)}); k = 1, \dots, K)^{\mathsf{T}} \in \mathbb{R}^q$ as the estimator obtained at the tth iteration on the mth client. Additionally, define the corresponding whole sample estimator and the true parameter as $\widehat{\psi} = (\widehat{\alpha}_k, \widehat{\alpha}_k(\widehat{\mu}_k)^{\mathsf{T}}, \widehat{\alpha}_k \, \mathrm{vech}^{\mathsf{T}}(\widehat{\Sigma}_k); k = 1, \dots, K)^{\mathsf{T}}$ and $\psi_0 = (\alpha_k, \alpha_k(\mu_k)^{\mathsf{T}}, \alpha_k \, \mathrm{vech}^{\mathsf{T}}(\Sigma_k); k = 1, \dots, K)^{\mathsf{T}}$. We aim to establish the oracle property of $\widehat{\psi}_{\mathrm{mnem}}^{(t,m)}$, meaning that the difference between $\widehat{\psi}_{\mathrm{mnem}}^{(t,m)}$ and the whole sample estimator $\widehat{\psi}$ is asymptotically negligible. Here, we discuss the theoretical properties of $\widehat{\psi}_{\mathrm{mnem}}^{(t,m)}$ instead of $\widehat{\theta}_{\mathrm{mnem}}^{(t,m)}$. Notice that $\widehat{\psi}_{\mathrm{mnem},k}^{(t,m)}$ is a linear transformation of $\widehat{\theta}_{\mathrm{mnem},k}^{(t,m)}$. Therefore, the theoretical property of $\widehat{\theta}_{\mathrm{mnem}}^{(t,m)}$ can be readily derived based on that of $\widehat{\psi}_{\mathrm{mnem}}^{(t,m)}$. To build intuition and explain why the MNEM estimator achieves the oracle property, we rewrite each iteration as $\widehat{\psi}_{\mathrm{mnem}}^{(t+1,m)} = (1-\eta)\widehat{\psi}_{\mathrm{mnem}}^{(t,m)} + \eta \mathcal{F}_{(m)}(\widehat{\psi}_{\mathrm{mnem}}^{(t,m)})$ where $\widehat{\psi}_{\mathrm{mnem}}^{(t,m)}$ denotes the neighborhood-averaged estimator and the detailed definition of the mapping function $\mathcal{F}_{(m)}(\cdot)$ is given in Appendix. Similar to (2.4), we have by Taylor's expansion that

$$\widehat{\psi}_{\text{mnem}}^{(t+1,m)} - \widehat{\psi} \approx \left[1 - \eta \left\{1 - \dot{\mathcal{F}}_{(m)}(\psi_0)\right\}\right] \left(\widetilde{\psi}_{\text{mnem}}^{(t,m)} - \widehat{\psi}\right) + \eta \left\{\mathcal{F}_{(m)}(\widehat{\psi}) - \widehat{\psi}\right\}. \tag{3.3}$$

By equation (3.3), the discrepancy between $\widehat{\psi}_{\text{mnem}}^{(t+1,m)}$ and $\widehat{\psi}$ can be decomposed into two terms. The first term determines the numerical convergence property of the algorithm and depends on $\dot{\mathcal{F}}_{(m)}(\psi_0)$ and η . A contractive $\dot{\mathcal{F}}_{(m)}(\psi_0)$ ensures its numerical convergence. The second term determines the statistical properties of the estimator. With heterogeneous data, $\mathcal{F}_{(m)}(\widehat{\psi})$ could differ significantly from $\widehat{\psi}$. However, it is important to note that the extra term diminishes by averaging since $M^{-1}\sum_{m=1}^{M}\mathcal{F}_{(m)}(\widehat{\psi})=\widehat{\psi}$. Therefore, by selecting a sufficiently small η , we can regulate the upper bound of this extra term. This guarantees that the MNEM estimator converges to the whole sample estimator, attaining the desired oracle property.

To formally MNEM's theoretical properties, we need to introduce some notations and regularity conditions. We begin with two metrics to measure the network structure. Define $\widehat{SE}^2(W) = M^{-1} \|W^{\mathsf{T}} \mathbf{1}_M - \mathbf{1}_M\|^2$, which calculates the variance of the column sums of matrix W and thus measures the balance of network structures. By definition, a smaller $\widetilde{SE}(W)$ value implies a more balanced network. In the most ideal situation where W is doubly stochastic in the sense that $\mathbf{1}_M^{\mathsf{T}}W = \mathbf{1}_M^{\mathsf{T}}$ (Yuan et al., 2016; Lian et al., 2018; Li et al., 2019b), we have $\widehat{SE}(W) = 0$. Next, define $\sigma_w^2 = \|W^{\mathsf{T}}(I_M - M^{-1}\mathbf{1}_M\mathbf{1}_M^{\mathsf{T}})W\|$, where $\|B\| = \lambda_{\max}(B^{\mathsf{T}}B)$ represents the ℓ_2 norm for a matrix B. This metric is closely related to the numerical convergence rate of a sequence W^t to its limit as $t \to \infty$. To illustrate this point, again, assume W is a doubly stochastic matrix. It follows that $\|W^{t+1} - W^{\infty}\| \le \sigma_w^t \|W - W^{\infty}\|$. Thus a smaller σ_w suggests that W can converge to W^{∞} at a faster speed. Moreover, define $\widehat{SE}^2(\mathcal{F}) = M^{-1} \sum_{m=1}^M \|\mathcal{F}_{(m)}(\widehat{\psi}) - \mathcal{F}(\widehat{\psi})\|^2$ for the mapping function \mathcal{F} and $\mathcal{F}(\psi) = M^{-1} \sum_{m=1}^{M} \mathcal{F}_{(m)}(\psi)$, which measures the data heterogeneity to some extent. When the data is homogeneous, we have $\widehat{SE}^2(\mathcal{F}) = O_p(1/n)$. By contrast, a larger $\widetilde{\mathrm{SE}}(\mathcal{F})$ value indicates a more heterogeneous data distribution (Lian et al., 2018; Wu et al., 2023). We then require the following conditions to hold:

- (C2.a) (SMOOTHNESS) For any $1 \le m \le M$, there exists some positive constant L_{\max} such that $\|\mathbb{E}\{\dot{\mathcal{F}}_{(m)}(\psi')\}\| \le L_{\max}$ for any $\psi' \in B(\psi_0, \delta)$.
 - (C3) (Degree of Separation) Define $\bar{L}_{\max} = \|\mathbb{E}\{\dot{\mathcal{F}}(\psi_0)\}\|$, assume $\bar{L}_{\max} < 1$.
 - (C4) (DATA GENERATING PROCESS) Assume that the local data $\{X_i\}_{i\in\mathcal{S}_m}$ on the mth client are independently and identically distributed from an unknown sub-Gaussian distribution $\mathcal{P}_{(m)}$.
 - (C5) (Network Structure) Define $\rho_w = \sigma_w + \widehat{SE}(W)$, assume $\rho_w < 1$.

Condition (C3) imposes specific requirements on the degree of separation between the mixture components. For technical convenience, we assume $\|\mathbb{E}\{\dot{\mathcal{F}}(\psi_0)\}\| < 1$ instead of $\tau_k < \alpha_k(1-\alpha_k)$ for $1 \le k \le K$. We can rigorously prove that (C3) is indeed satisfied under certain conditions. In addition, it is important to note that we only require the whole sample mapping function $\dot{\mathcal{F}}(\cdot)$ to be contractive on ψ_0 . This assumption is milder than requiring $\dot{\mathcal{F}}_{(m)}(\cdot)$ for each m to be contractive. The latter is widely used in the existing DFL literature (Shi et al., 2015; Yuan et al., 2016). Condition (C4) allows the data to be heterogeneous across different clients (Gu and Chen, 2023). Condition (C5) imposes restrictions on the network structure. It is weaker than existing conditions in the literature, which require W to be a doubly stochastic matrix (Li et al., 2019b; Song et al., 2023). This relaxation enables us to study the impact of network topology on the algorithm.

Finally, write $\widehat{\psi}_{\mathrm{mnem}}^{*(t)} = \{(\widehat{\psi}_{\mathrm{mnem}}^{(t,1)})^{\mathsf{T}}, \dots, (\widehat{\psi}_{\mathrm{mnem}}^{(t,M)})^{\mathsf{T}}\}^{\mathsf{T}} \in \mathbb{R}^{Mq} \text{ and } \widehat{\psi}^* = I^*\widehat{\psi} \in \mathbb{R}^{Mq} \text{ as the stacked MNEM estimator and whole sample estimator, respectively. Let } \widehat{\delta}_0 = \|\widehat{\psi}_{\mathrm{mnem}}^{(0,m)} - \widehat{\psi}\|$ represent the estimation error due to the initial estimator. For simplicity, we assume that all clients start from the same initial value $\widehat{\delta}_0$. We then present the following theorem.

Theorem 3. Assume that conditions (C1),(C2.a),(C3)-(C5) hold. Further assume that $\eta + \widehat{SE}(W)$ is sufficiently small and the initial value $\widehat{\psi}_{mnem}^{*(0)}$ is sufficiently close to $\widehat{\psi}^*$ in a sense $\eta + \widehat{SE}(W) < \epsilon$ and $\|\widehat{\delta}_0\| \le \epsilon$ for some sufficiently small but fixed positive constant ϵ . Then $M^{-1/2}\|\widehat{\psi}_{mnem}^{*(t)} - \widehat{\psi}^*\|$ is upper bounded by

$$C_{2}\left[\left\{1-\frac{\eta}{2}\left(1-\bar{L}_{\max}\right)\right\}^{t-1}\widehat{\delta}_{0}+\frac{\eta+\widehat{SE}(W)}{\left(1-\bar{L}_{\max}\right)(1-\rho_{w})}\widehat{SE}(\mathcal{F})+\frac{\left\{\eta+\widehat{SE}(W)\right\}^{2}}{\left(1-\bar{L}_{\max}\right)^{2}(1-\rho_{w})^{2}}\right] (3.4)$$

with probability at least $1 - O(Mn^{-\alpha})$ for any $\alpha \ge 1$ and some fixed constant C_2 . Here C_2 depends on α but is independent of (\bar{L}_{\max}, n, M) . In particular, when $\eta + \widehat{SE}(W) = o_p(N^{-1/2})$, the MNEM estimator possesses the oracle property.

Theorem 3 decomposes the estimation error of MNEM into two parts. The first part is the numerical error due to $\widehat{\delta}_0$, which converges linearly towards 0. This error is mainly determined by the momentum parameter η and the separability of the Gaussian components characterized by $\overline{L}_{\text{max}}$. Specifically, a smaller $\overline{L}_{\text{max}}$ value and a larger η value indicate faster numerical convergence. The second part is the statistical error, which is mainly controlled by the following factors: the momentum parameter η , the network structure $\widehat{\text{SE}}(W)$, the data heterogeneity measured by $\widehat{\text{SE}}(\mathcal{F})$, and the degree of separation represented by $\overline{L}_{\text{max}}$. By (3.4), the following factors contribute to improving statistical efficiency: (i) a smaller momentum parameter η ; (ii) a more balanced network structure W; (iii) more separable Gaussian components (i.e., a smaller $\overline{L}_{\text{max}}$ value); and (iv) a more homogeneous data distribution (i.e., a smaller $\widehat{\text{SE}}(\mathcal{F})$ value).

Furthermore, the MNEM estimator can be asymptotically as effective as the whole sample estimator, as long as

$$\frac{\eta + \widehat{SE}(W)}{\left(1 - \bar{L}_{\max}\right)(1 - \rho_w)} \widehat{SE}(\mathcal{F}) + \frac{\left\{\eta + \widehat{SE}(W)\right\}^2}{\left(1 - \bar{L}_{\max}\right)^2 (1 - \rho_w)^2} = o_p(N^{-1/2}). \tag{3.5}$$

A sufficient condition for (3.5) is that $\eta + \widehat{SE}(W) = o_p(N^{-1/2})$. As a consequence, incorporating the momentum method into the EM algorithm enables the resulting estimator to achieve the oracle property, even when data is heterogeneous across different clients.

3.4. Theoretical Properties of the semi-MNEM

In this section, we establish the theoretical properties of the semi-MNEM. To this end, define $\widehat{\psi}_{\text{snem}}^{(t,m)} = (\widehat{\alpha}_{\text{snem},k}^{(t,m)}, (\widehat{\beta}_{\text{snem},k}^{(t,m)})^{\intercal}, \text{vech}^{\intercal}(\widehat{\gamma}_{\text{snem},k}^{(t,m)}); k = 1, \dots, K)^{\intercal} \in \mathbb{R}^{q}$. Given the neighborhood-averaged estimator $\widetilde{\psi}_{\text{snem}}^{(t,m)}$, each iteration can be represented as $\widetilde{\psi}_{\text{snem}}^{(t+1,m)}$ = $(1-\eta)\widetilde{\psi}_{\text{snem}}^{(t,m)} + \eta \mathsf{F}_{(m)}(\widetilde{\psi}_{\text{snem}}^{(t,m)})$ for some properly chosen mapping function $\mathsf{F}_{(m)}(\cdot)$; refer its specific definition in Appendix. Compared to the MNEM algorithm, it can be verified that $\|\dot{\mathsf{F}}_{(m)}(\psi_0)\| < \|\dot{\mathcal{F}}_{(m)}(\psi_0)\|$, suggesting that semi-MNEM converges faster than MNEM. Here we illustrate this point informally using the derivative of the operators at α_k as an example. The formal conclusion is presented in the subsequent theorem. Specifically, it can be verified that the components of $F_{(m)}(\psi_0)$ and $\mathcal{F}_{(m)}(\psi_0)$ at α_k are given by $\left(\sum_{i \in \mathcal{S}_m \setminus \mathcal{S}_m^*} \pi_{ik} + \sum_{i \in \mathcal{S}_m^*} a_{ik}\right)/n$ and $\sum_{i \in \mathcal{S}_m} \pi_{ik}/n$, respectively. Note that: (i) $\sum_{i \in \mathcal{S}_m \setminus \mathcal{S}_m^*} \pi_{ik}$ is only a subset of $\sum_{i \in \mathcal{S}_m} \pi_{ik}$ and (ii) a_{ik} does not include the unknown parameters of interest, thus its derivative with respect to the parameters is zero. As a result, semi-MNEM can effectively mitigate the numerical convergence challenges encountered by the MNEM, particularly when the Gaussian components are poorlyseparated. To explore the theoretical properties of the semi-MNEM, we introduce the following regularity condition.

(C2.b) (SMOOTHNESS) For any $1 \le m \le M$, there exists some positive constant L_{\max} such that $\|\mathbb{E}\{\dot{\mathsf{F}}_{(m)}(\psi')\}\| \le L_{\max}$ for any $\psi' \in B(\psi_0, \delta)$.

Finally, denote $\bar{L}_{\max}^{\text{semi}} = \|\mathbb{E}\{\dot{\mathsf{F}}(\psi_0)\}\|$, $\widehat{\psi}_{\text{snem}}^{\star(t)} = \{(\widehat{\psi}_{\text{snem}}^{(t,1)})^{\mathsf{T}}, \dots, (\widehat{\psi}_{\text{snem}}^{(t,M)})^{\mathsf{T}}\}^{\mathsf{T}} \in \mathbb{R}^{Mq}$ as the stacked semi-MNEM estimate obtained in the tth iteration. Write $\widehat{\psi}_{\text{semi}}$ and $\widehat{\psi}_{\text{semi}}^{\star} = 0$

 $I^*\widehat{\psi}_{\text{semi}} \in \mathbb{R}^{Mq}$ as the whole sample estimator and its stacked counterpart respectively. We summarize our results in the following theorem.

Theorem 4. Assume conditions (C1), (C2.b), (C4), and (C5) hold. Further assume that $\eta + \widehat{SE}(W)$ is sufficiently small, and the initial value $\widehat{\psi}_{\text{snem}}^{*(0)}$ is sufficiently close to $\widehat{\psi}_{\text{semi}}^{*}$ in the sense $\eta + \widehat{SE}(W) < \epsilon$ and $\|\widehat{\delta}_{0}^{\dagger}\| \le \epsilon$ for some sufficiently small but fixed positive constant ϵ with $\widehat{\delta}_{0}^{\dagger} = \|\widehat{\psi}_{\text{snem}}^{(0,m)} - \widehat{\psi}_{\text{semi}}\|$. We then have $\overline{L}_{\text{max}}^{\text{semi}} = (1 - n^*/n) \overline{L}_{\text{max}}$. Furthermore, for a sufficiently large n^* , we have $\overline{L}_{\text{max}}^{\text{semi}} < 1$, and $M^{-1/2} \|\widehat{\psi}_{\text{snem}}^{*(t)} - \widehat{\psi}_{\text{semi}}^{*}\|$ is upper bounded by

$$C_{3} \left[\left\{ 1 - \frac{\eta}{2} \left(1 - \bar{L}_{\max}^{\text{semi}} \right) \right\}^{t-1} \widehat{\delta}_{0}^{\dagger} + \frac{\eta + \widehat{\text{SE}}(W)}{\left(1 - \bar{L}_{\max}^{\text{semi}} \right) (1 - \rho_{w})} \widehat{\text{SE}}(\mathsf{F}) + \frac{\left\{ \eta + \widehat{\text{SE}}(W) \right\}^{2}}{\left(1 - \bar{L}_{\max}^{\text{semi}} \right)^{2} (1 - \rho_{w})^{2}} \right]$$
(3.6)

with probability at least $1 - O(Mn^{-\alpha})$ for any $\alpha \ge 1$ and some constant $C_3 > 0$. Here C_3 is related to α but independent of $(\bar{L}_{\max}^{\text{semi}}, n, M)$. In particular, when $\eta + \widehat{SE}(W) = o_p(N^{-1/2})$, the semi-MNEM estimator possesses the oracle property.

Comparing Equation (3.6) against (3.4), we observe that the primary distinction lies in the value of $\bar{L}_{\rm max}^{\rm semi}$ in (3.6) being smaller than $\bar{L}_{\rm max}$ in (3.4), due to the incorporation of additional label information. This leads to two important conclusions: (i) Compared to the MNEM, the semi-MNEM achieves better statistical estimation efficiency; (ii) Even with poorly-separated Gaussian components, the incorporation of label information forces the contraction operator $\bar{L}_{\rm max}^{\rm semi}$ to remain well below 1. This substantially enhances the numerical convergence of semi-MNEM, effectively addressing challenges associated with poorly-separated Gaussian components.

4. NUMERICAL STUDIES

4.1. The Basic Setups

To evaluate the finite sample performance of the proposed methods (i.e., the NNEM, MNEM, and semi-MNEM methods), we present a number of numerical studies on both simulated and real datasets. For the simulation studies, we set the feature dimension as p=6, the category size as K=3, the sample size as N=30,000, and the number of clients as M=20. Therefore, the sample size for each client is given by n=1,500. We next generate Y_i according to $\mathbb{P}(Y_i=k)=\alpha_k$ for $1\leq k\leq 3$ with $\alpha_1=0.5$, $\alpha_2=0.3$, and $\alpha_3=0.2$. Given $Y_i=k$, X_i is then generated from the multivariate Gaussian distribution $N_p(\mu_k, \Sigma_k)$. Here, $\Sigma_k=(\sigma_{k,ij})$ with $\sigma_{k,ij}=\rho_k^{|i-j|}$, where $\rho_1=0.5$, $\rho_2=0.1$, and $\rho_3=-0.1$. For the conditional mean, we generate $\mu_1\sim N_p(0,I_p)$ and set $\mu_k=\mu_{k-1}+C\mathbf{1}_p$ for $k\in\{2,3\}$. Note that a larger C value implies a smaller value of τ_k , thus the constant C controls the degree of separation. In this study, we set $C\in\{1,2,4\}$. Moreover, set $r=n^*/n\in\{0,0.05,0.10,0.50,1\}$ be the proportion of the labeled samples. The cases with r=0 correspond to the fully unsupervised methods (i.e., the NNEM and MNEM methods) while the cases with r>0 correspond to the semi-MNEM method.

After the observations are generated, they are distributed to different clients. We consider two different data generating processes. The first is the homogeneous process, where all observations are distributed to different clients in a completely random manner. The second is the heterogeneous process, where all observations are sorted according to their response values. These sorted observations are then distributed sequentially to different clients, resulting in similar label values for the observations assigned to the same clients. In addition, three different network structures are considered, namely, the star network structure, the fixed-degree network structure, and the circle-type network structure. The details of these network structures are presented in Appendix. It can be verified that the circle-type network structure is the most balanced with $\widehat{SE}(W) = 0$, while the star network structure is the most unbalanced with $\widehat{SE}(W) = (M-2)/(M-1)^{1/2}$. Finally, we set the momentum parameter

 $\eta \in \{0.01, 0.02, 0.05\}$ for MNEM and semi-MNEM.

For each simulation study, the experiments are replicated a total of R=100 times for each parameter setup. Let $\widehat{\theta}_s^{(t,m)}$ be the estimator obtained on the mth client in the sth replicate on the tth iteration. We then compute the mean squared error (MSE) values to evaluate the finite sample performance, defined as MSE = $\{MR\}^{-1}\sum_{s=1}^{R}\sum_{m=1}^{M}\|\widehat{\theta}_s^{(t,m)}-\theta_0\|^2$. In addition to the proposed methods, the MSE values of the local optimal estimator $\widehat{\theta}_{loc}$ (i.e., "Local"), the whole sample optimal estimator $\widehat{\theta}$ in the unsupervised case (i.e., "EM"), and the whole sample optimal estimator $\widehat{\theta}_{seni}$ in the semi-supervised case (i.e., "semi-EM") are shown as reference information. We report the mean log(MSE) values of MNEM and semi-MNEM in Figure 1. In the main text, we fix the network structure to a circle-type network and set the momentum to $\eta=0.01$. The primary focus is on the effect of data generating processes and the degree of separation on the proposed estimators. Results under different network structures and momentum parameters for MNEM and semi-MNEM, as well as results for NNEM, are presented in Appendix. Additionally, complete implementation details are also provided in Appendix.

Figure 1 shows the following interesting findings. First, when C = 2 and C = 4, both MNEM and semi-MNEM converge to the whole sample estimator, even if the data generating process across different clients is heterogeneous. This result is consistent with our theoretical findings in Theorem 3. Second, when C = 1, MNEM suffers from a painfully slow convergence speed. This convergence issue can be resolved by the semi-MNEM method with a small labeled ratio (i.e., r = 0.05). Finally, the convergence speed and statistical efficiency of semi-MNEM increase with increasing r. These findings corroborate our theoretical results in Theorem 4.

4.2. Comparison with Competing Methods

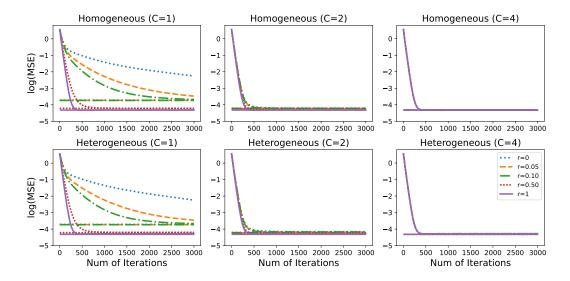


Figure 1: The $\log(\text{MSE})$ values of MNEM and EM (r=0), as well as semi-MNEM and semi-EM (r>0) for the circle-type network structure. Each r value corresponds to two lines, where the curve represents the proposed method MNEM or semi-MNEM and the line represents the whole sample estimator EM or semi-EM. The upper and lower panels represent the homogeneous and heterogeneous data generating process respectively. The left, middle, and right panels represent C=1,2,4 respectively.

For a more comprehensive comparison, we next compare the proposed estimators with two competing methods. The first method is the existing distributed EM algorithm over sensor networks (DEM) from Gu (2008). The second method uses the decentralized network gradient descent (NGD) method instead of EM method to estimate parameters in GMM (Yuan et al., 2016; Wu et al., 2023). It is important to note that both competing methods can be easily extended from fully unsupervised GMM to partially labeled scenarios. Therefore, we also compare how these competing methods perform when the data is partially labeled. We denote the resulting estimators as semi-DEM and semi-NGD.

The simulation model used here is the same as that in Section 5.1. In particular, we fix the labeled ratio at r = 0.1 and the network structure to be a circle-type network. Remarkably, both the NGD and semi-NGD methods are highly sensitive to the learning rate, which plays a similar role to that of η in the MNEM method. These methods may

fail to achieve numerical convergence when η is relatively large. Therefore, two different η values are carefully set for (semi-)NGD. We set $\eta=0.05,0.15$ for the homogeneous process and $\eta=0.001,0.003$ for the heterogeneous process. For the other methods, we fix $\eta=0.01$. The log(MSE) values of MNEM, DEM, and NGD are summarized in Figure 2. The log(MSE) values of semi-MNEM, semi-DEM, and semi-NGD are given in Figure 3.

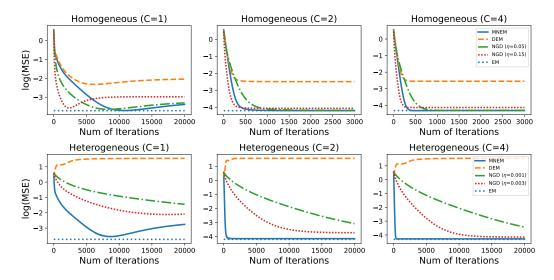


Figure 2: The log(MSE) values of MNEM, DEM, and NGD for different distribution patterns and separabilities of Gaussian components. The blue dotted line represents the whole sample EM estimators. Here, we fix the network structure to be a circle-type structure and $\eta=0.01$ for MNEM and DEM.

We obtained several interesting findings from Figure 2. First, in the homogeneous case, all methods converge when the C is relatively large. Among these, the NGD method with $\eta = 0.15$ exhibits the fastest convergence rate. The convergence speed of MNEM is comparable to that of NGD at $\eta = 0.15$ and higher than those of the other two methods. Additionally, DEM yields the highest MSE, while the remaining methods obtain results similar to those of the whole sample EM estimator. When the data is poorly-separated, only the DEM and NGD methods achieve convergence at T = 20,000 steps, yet their MSE values are significantly greater than the whole sample MSE. In the heterogeneous scenario, MNEM outperforms all other methods when C

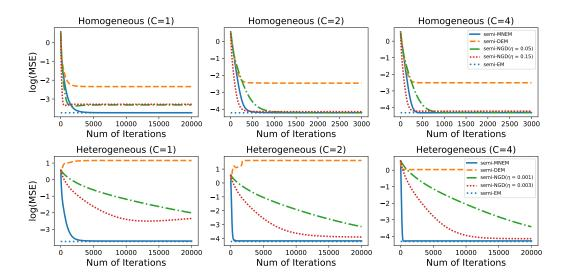


Figure 3: The log(MSE) values of semi-MNEM, semi-DEM, and semi-NGD for different distribution patterns and separabilities of Gaussian components. The blue dotted line represents the whole sample semi-EM estimators. Here, we fix the network structure to be a circle-type structure, the labeled ratio r = 0.1, and $\eta = 0.01$ for MNEM and DEM.

is relatively large, eventually achieving the same estimation accuracy as the whole sample optimum. However, when different mixture components are poorly-separated, none of the methods converge by T=20,000 steps. In summary, when the data is well-separated, MNEM is highly competitive with other methods in terms of convergence speed and attains the lowest MSE. Conversely, all methods underperform when the data is poorly-separated.

From Figure 3, we observe that qualitatively similar findings are obtained in both the C=2 and C=4 cases. However, when the data is poorly-separated, we find that the performance of the semi-supervised methods improves compared to that of their unsupervised counterparts, primarily due to the use of partially labeled data. Among these methods, semi-MNEM achieves the smallest MSE which is comparable to the whole sample estimator, and exhibits the fastest convergence speed.

4.3. Real Data Analysis

To demonstrate the practical performance of the proposed methods, we provide a real-world example using the MNIST dataset of handwritten digits (LeCun et al., 1998). This dataset is available from the official website http://yann.lecun.com/exdb/mnist/. The MNIST dataset consists of 70,000 images of handwritten digits ranging from 0 to 9, with each digit category consisting of approximately 7,000 images. A total of 60,000 of these images are allocated for training purposes, while the remaining 10,000 images are reserved for validation.

In the MNIST dataset, the images serve as our features. Assuming that the labels are unobserved, we can employ a GMM to analyze the data (Tian et al., 2023). The original MNIST images are 28×28 -dimensional grayscale images. To simplify our analysis, we apply PCA to reduce their dimensionality. Specifically, we set the cumulative variance contribution rate to 70%, which results in a dimensionality reduction to p = 26 dimensions. Subsequently, to train the model, we distribute the training data across M = 10 clients. Here we consider two types of data generating processes. The first is the homogeneous pattern, where data is randomly distributed across 10 clients. The second is the heterogeneous pattern, where each client handles only one class of data. Thus, this distribution strategy introduces extreme heterogeneity across clients. The initial values for each algorithm are set based on preliminary K-means clustering; see the detailed implementation in Appendix.

This section compares two proposed methods (i.e., NNEM and MNEM) and two competing methods (i.e., DEM and NGD). For the MNEM, DEM, and NGD methods, we also consider their semi-supervised counterparts. The experimental settings are consistent with those described in Section 5.2. Since the ground truth is unknown in real data analysis, we evaluate the prediction performance using the mis-clustering error rate, denoted as Err(t,m), on the validation set. Specifically, we define Y_i^{val} as the true label and Y_i^{pred} as the label predicted by a specific method for the ith validation

set. The error rate, Err(t, m), is calculated as follows:

$$\operatorname{Err}(t,m) = \frac{1}{N_{\text{val}}} \sum_{i=1}^{N_{\text{val}}} I\left\{Y_i^{\text{pred}} \neq \pi(Y_i^{\text{val}})\right\},\,$$

where $N_{\text{val}} = 10,000$ represents the total number of samples in the validation dataset, and π is a permutation function used to match the predicted labels with the true labels. For each t, we can obtain M Err-values, their means, and log-transformed standard deviations are reported in the bar plots presented in Figure 4.

From Figures 4, we derive the following interesting findings. In the homogeneous case, NNEM, DEM, and MNEM show comparable performance. By the 1,000th iteration, their mis-clustering rates align with those of the whole sample version. The NGD method exhibits minimal convergence within the first 1,000 steps. Furthermore, with partial labeling, the convergence speeds of the DEM and MNEM algorithms improve significantly, resulting in lower final mis-clustering rates. In the heterogeneous case, the situation differs significantly. In this scenario, NNEM, NGD, and DEM fail to converge, with NNEM exhibiting the worst performance. Conversely, MNEM demonstrates superior performance, matching that of the optimal estimator. Similar results are observed in the semi-supervised scenario.

5. CONCLUDING REMARKS

We study the Gaussian Mixture Model within a DFL framework. Our preliminary analysis reveals that extending supervised DFL methods to the EM algorithm may result in significant bias with heterogeneous data generating processes and struggle to converge with poorly-separated Gaussian components. To address the issue of heterogeneity, we introduce the NEM algorithm with momentum (i.e., MNEM) and demonstrate that, MNEM can achieve performance asymptotically comparable to the

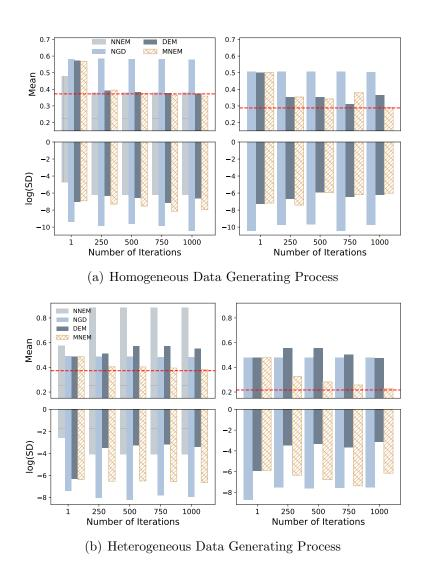


Figure 4: The mean and log(SD) for the Err values obtained by different estimators. The left panel represents the original GMM model, while the right panel shows the results for the counterparts of NGD, DEM, and MNEM with partial labeling. Here, we fix the network structure to be a circle-type structure with a proportion of 10% instances labeled. Moreover, the red dotted line in the upper panel represents the optimal Err value, which is calculated based on the entire dataset using a single computer.

whole sample estimator, provided the momentum parameter is sufficiently small and the Gaussian components satisfy certain separation conditions. Furthermore, to resolve the problem of poorly-separated Gaussian components, we propose the partially labeled semi-MNEM method, which enhances the convergence speed of MNEM significantly. Extensive numerical studies are presented to demonstrate the finite sample performance. To conclude this article, we discuss several intriguing topics for future

study. First, all three of our proposed methods require the transmission of covariance matrices, which can lead to high communication costs in high-dimensional settings. The development of more communication-efficient and decentralized EM algorithms should be the subject of further study. Second, our work focuses solely on the GMM model. Extending these methods to more general unsupervised models presents an interesting research problem for future investigations.

REFERENCES

- Bellet, A., Guerraoui, R., Taziki, M., and Tommasi, M. (2018), "Personalized and private peer-to-peer machine learning," in *International Conference on Artificial Intelligence and Statistics*, PMLR, pp. 473–481.
- Blot, M., Picard, D., Cord, M., and Thome, N. (2016), "Gossip training for deep learning," arXiv preprint arXiv:1611.09726.
- Boldea, O. and Magnus, J. R. (2009), "Maximum likelihood estimation of the multivariate normal mixture model," *Journal of the American Statistical Association*, 104, 1539–1549.
- Chen, X., Liu, W., and Zhang, Y. (2022), "First-order newton-type estimator for distributed estimation and inference," *Journal of the American Statistical Association*, 117, 1858–1874.
- Chen, X. and Xie, M.-g. (2014), "A split-and-conquer approach for analysis of extraor-dinarily large data," *Statistica Sinica*, 1655–1684.
- Colin, I., Bellet, A., Salmon, J., and Clémençon, S. (2016), "Gossip dual averaging for decentralized optimization of pairwise functions," in *International Conference on Machine Learning*, PMLR, pp. 1388–1396.
- Cozman, F. G., Cohen, I., Cirelo, M. C., et al. (2003), "Semi-supervised learning of mixture models," in *ICML*, vol. 4, p. 24.

- Dempster, A. P., Laird, N. M., and Rubin, D. B. (1977), "Maximum likelihood from incomplete data via the EM algorithm," *Journal of the royal statistical society: series B (methodological)*, 39, 1–22.
- Fan, J., Guo, Y., and Wang, K. (2023), "Communication-efficient accurate statistical estimation," *Journal of the American Statistical Association*, 118, 1000–1010.
- Fang, X. and Ye, M. (2022), "Robust federated learning with noisy and heterogeneous clients," in *Proceedings of the IEEE/CVF Conference on Computer Vision and Pattern Recognition*, pp. 10072–10081.
- Gabrielli, E., Pica, G., and Tolomei, G. (2023), "A survey on decentralized federated learning," arXiv preprint arXiv:2308.04604.
- Gu, D. (2008), "Distributed EM algorithm for Gaussian mixtures in sensor networks," *IEEE Transactions on Neural Networks*, 19, 1154–1166.
- Gu, J. and Chen, S. X. (2023), "Statistical Inference for Decentralized Federated Learning," Working Paper.
- Han, L., Hou, J., Cho, K., Duan, R., and Cai, T. (2021), "Federated adaptive causal estimation (face) of target treatment effects," arXiv preprint arXiv:2112.09313.
- Hathaway, R. J. (1985), "A constrained formulation of maximum-likelihood estimation for normal mixture distributions," *The Annals of Statistics*, 795–800.
- Hector, E. C. and Song, P. X.-K. (2021), "A distributed and integrated method of moments for high-dimensional correlated data analysis," *Journal of the American Statistical Association*, 116, 805–818.
- Heinrich, P. and Kahn, J. (2018), "Strong identifiability and optimal minimax rates for finite mixture estimation,".
- Jordan, M. I., Lee, J. D., and Yang, Y. (2019), "Communication-efficient distributed statistical inference," *Journal of the American Statistical Association*, 114, 668–681.

- Kairouz, P., McMahan, H. B., Avent, B., Bellet, A., Bennis, M., Bhagoji, A. N., Bonawitz, K., Charles, Z., Cormode, G., Cummings, R., et al. (2021), "Advances and open problems in federated learning," Foundations and Trends® in Machine Learning, 14, 1–210.
- Kiefer, N. M. (1978), "Discrete parameter variation: Efficient estimation of a switching regression model," *Econometrica: Journal of the Econometric Society*, 427–434.
- Konečný, J., McMahan, H. B., Yu, F. X., Richtárik, P., Suresh, A. T., and Bacon, D. (2016), "Federated learning: Strategies for improving communication efficiency," arXiv preprint arXiv:1610.05492.
- Kwon, J. and Caramanis, C. (2020), "The EM algorithm gives sample-optimality for learning mixtures of well-separated gaussians," in *Conference on Learning Theory*, PMLR, pp. 2425–2487.
- LeCun, Y., Bottou, L., Bengio, Y., and Haffner, P. (1998), "Gradient-based learning applied to document recognition," *Proceedings of the IEEE*, 86, 2278–2324.
- Li, T., Sahu, A. K., Zaheer, M., Sanjabi, M., Talwalkar, A., and Smith, V. (2020), "Federated optimization in heterogeneous networks," *Proceedings of Machine learn-ing and systems*, 2, 429–450.
- Li, X., Huang, K., Yang, W., Wang, S., and Zhang, Z. (2019a), "On the Convergence of FedAvg on Non-IID Data," in *International Conference on Learning Representations*.
- Li, Y., Chen, C., Liu, N., Huang, H., Zheng, Z., and Yan, Q. (2021), "A Blockchain-Based Decentralized Federated Learning Framework with Committee Consensus," IEEE Network, 35, 234–241.
- Li, Z., Shi, W., and Yan, M. (2019b), "A decentralized proximal-gradient method with network independent step-sizes and separated convergence rates," *IEEE Transactions on Signal Processing*, 67, 4494–4506.

- Lian, X., Zhang, C., Zhang, H., Hsieh, C.-J., Zhang, W., and Liu, J. (2017), "Can decentralized algorithms outperform centralized algorithms? a case study for decentralized parallel stochastic gradient descent," arXiv preprint arXiv:1705.09056.
- Lian, X., Zhang, W., Zhang, C., and Liu, J. (2018), "Asynchronous decentralized parallel stochastic gradient descent," in *International Conference on Machine Learning*, PMLR, pp. 3043–3052.
- Liu, W., Chen, L., Chen, Y., and Zhang, W. (2020), "Accelerating federated learning via momentum gradient descent," *IEEE Transactions on Parallel and Distributed* Systems, 31, 1754–1766.
- Liu, W., Chen, L., and Zhang, W. (2022), "Decentralized federated learning: Balancing communication and computing costs," *IEEE Transactions on Signal and Information Processing over Networks*, 8, 131–143.
- Ma, J., Xu, L., and Jordan, M. I. (2000), "Asymptotic convergence rate of the EM algorithm for Gaussian mixtures," *Neural Computation*, 12, 2881–2907.
- Marfoq, O., Neglia, G., Bellet, A., Kameni, L., and Vidal, R. (2021), "Federated multi-task learning under a mixture of distributions," *Advances in Neural Information Processing Systems*, 34, 15434–15447.
- McLachlan, G. J. and Basford, K. E. (1988), Mixture models: Inference and applications to clustering, vol. 38, M. Dekker New York.
- McLachlan, G. J., Lee, S. X., and Rathnayake, S. I. (2019), "Finite mixture models," Annual review of statistics and its application, 6, 355–378.
- McMahan, B., Moore, E., Ramage, D., Hampson, S., and y Arcas, B. A. (2017), "Communication-efficient learning of deep networks from decentralized data," in *Artificial intelligence and statistics*, PMLR, pp. 1273–1282.
- Regev, O. and Vijayaraghavan, A. (2017), "On learning mixtures of well-separated gaussians," in 2017 IEEE 58th Annual Symposium on Foundations of Computer Science (FOCS), IEEE, pp. 85–96.

- Reynolds, D. A. et al. (2009), "Gaussian mixture models." *Encyclopedia of biometrics*, 741.
- Safarinejadian, B., Menhaj, M. B., and Karrari, M. (2010), "A distributed EM algorithm to estimate the parameters of a finite mixture of components," *Knowledge and information systems*, 23, 267–292.
- Sattler, F., Wiedemann, S., Müller, K.-R., and Samek, W. (2019), "Robust and communication-efficient federated learning from non-iid data," *IEEE transactions on neural networks and learning systems*, 31, 3400–3413.
- Shi, C., Lu, W., and Song, R. (2018a), "A massive data framework for M-estimators with cubic-rate," *Journal of the American Statistical Association*, 113, 1698–1709.
- Shi, C., Song, R., Lu, W., and Fu, B. (2018b), "Maximin projection learning for optimal treatment decision with heterogeneous individualized treatment effects," *Journal of the Royal Statistical Society Series B: Statistical Methodology*, 80, 681–702.
- Shi, W., Ling, Q., Wu, G., and Yin, W. (2015), "Extra: An exact first-order algorithm for decentralized consensus optimization," *SIAM Journal on Optimization*, 25, 944–966.
- Song, Z., Shi, L., Pu, S., and Yan, M. (2023), "Optimal gradient tracking for decentralized optimization," *Mathematical Programming*, 1–53.
- Stich, S. U. (2018), "Local SGD converges fast and communicates little," arXiv preprint arXiv:1805.09767.
- Tang, K., Liu, W., and Mao, X. (2024), "Multi-consensus decentralized primal-dual fixed point algorithm for distributed learning," *Machine Learning*, 1–43.
- Tian, Y., Weng, H., and Feng, Y. (2023), "Unsupervised Federated Learning: A Federated Gradient EM Algorithm for Heterogeneous Mixture Models with Robustness against Adversarial Attacks," arXiv preprint arXiv:2310.15330.

- Volgushev, S., Chao, S.-k., and Cheng, G. (2019), "Distributed inference for quantile regression processes," *The Annals of Statistics*, 47, 1634–1662.
- Wu, C. J. (1983), "On the convergence properties of the EM algorithm," *The Annals of statistics*, 95–103.
- Wu, S., Huang, D., and Wang, H. (2023), "Network gradient descent algorithm for decentralized federated learning," *Journal of Business & Economic Statistics*, 41, 806–818.
- Xiang, P., Zhou, L., and Tang, L. (2024), "Transfer learning via random forests: A one-shot federated approach," *Computational Statistics & Data Analysis*, 197, 107975.
- Xu, L. (1993), "Unsupervised learning by EM algorithm based on finite mixture of Gaussians," in World Congress on Neural Networks (Portland, OR), vol. 2, pp. 431–434.
- Xu, L. and Jordan, M. I. (1996), "On convergence properties of the EM algorithm for Gaussian mixtures," *Neural computation*, 8, 129–151.
- Yang, M.-S., Lai, C.-Y., and Lin, C.-Y. (2012), "A robust EM clustering algorithm for Gaussian mixture models," *Pattern Recognition*, 45, 3950–3961.
- Yuan, K., Ling, Q., and Yin, W. (2016), "On the convergence of decentralized gradient descent," SIAM Journal on Optimization, 26, 1835–1854.
- Zhang, Q. and Chen, J. (2022), "Distributed learning of finite gaussian mixtures," Journal of Machine Learning Research, 23, 1–40.
- Zhang, Y., Duchi, J. C., and Wainwright, M. J. (2013), "Communication-efficient algorithms for statistical optimization," *The Journal of Machine Learning Research*, 14, 3321–3363.
- Zhou, J., Hu, B., Feng, W., Zhang, Z., Fu, X., Shao, H., Wang, H., Jin, L., Ai, S., and Ji, Y. (2023), "An ensemble deep learning model for risk stratification of invasive lung adenocarcinoma using thin-slice CT," NPJ Digital Medicine, 6, 119.

Zhu, X., Li, F., and Wang, H. (2021), "Least-square approximation for a distributed system," *Journal of Computational and Graphical Statistics*, 30, 1004–1018.